Electronic Supplementary Material (ESI) for Nanoscale.


**Supporting Information for Nanoscale**

# Sodium Storage in Promising $MoS_2$-Carbon Anode: Elucidating Structural and Interfacial Transition in Intercalation Process and Conversion Reactions

*Rutao Wang,[a‡] Shijie Wang,[a‡] Dongdong Jin,[a] Yabin Zhang,[a] Xinyong Tao,[b] Li Zhang*[a]*

[a]Department of Mechanical and Automation Engineering, The Chinese University of Hong Kong, Shatin NT, Hong Kong SAR 999077, P. R. China.

[b]College of Materials Science and Engineering, Zhejiang University of Technology, Hangzhou 310014, P. R. China.

Email: lizhang@mae.cuhk.edu.hk

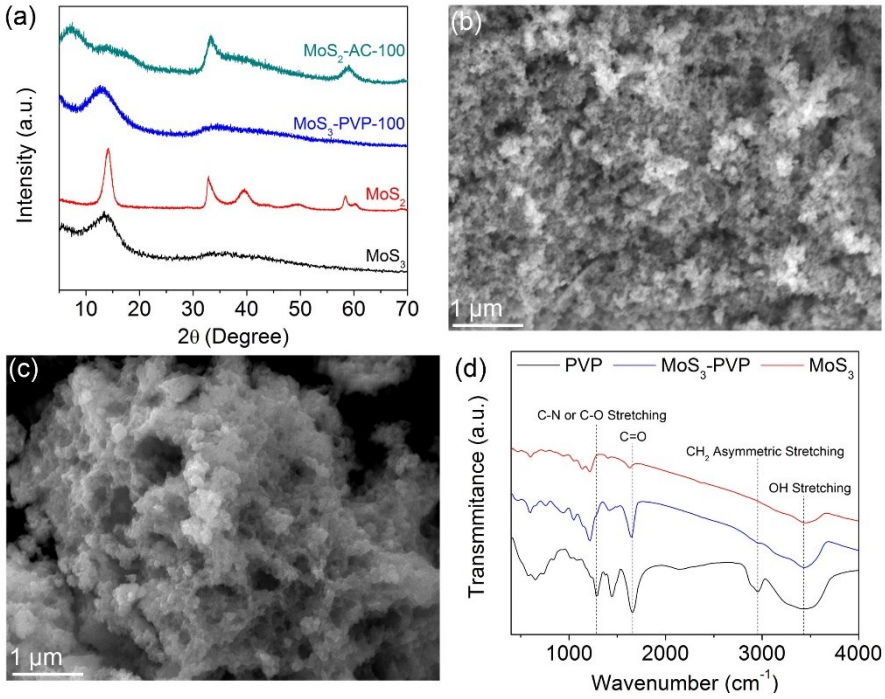


**Fig. S1** (a) XRD patterns of $MoS_3$ and $MoS_3$-PVP, (b) SEM image of $MoS_3$, (c) SEM image of $MoS_3$-PVP, (d) FTIR spectrum of PVP, $MoS_3$, $MoS_3$-PVP. $MoS_3$-PVP represents the precursor for $MoS_3$-AC-100 sample. The XRD patterns of $MoS_3$ and $MoS_3$-PVP show the typical profile of amorphous $MoS_3$. $MoS_3$ and $MoS_3$-PVP precursors display the granular morphology in nanosize.[S1,S2] The grain size of $MoS_3$-PVP is slightly larger than that of $MoS_3$, most likely due to PVP coating. The absorption peaks of FTIR from the chemical groups of PVP including C-N, C-O and $CH_2$ can be observed in $MoS_3$-PVP samples prepared with additional PVP.[S3]

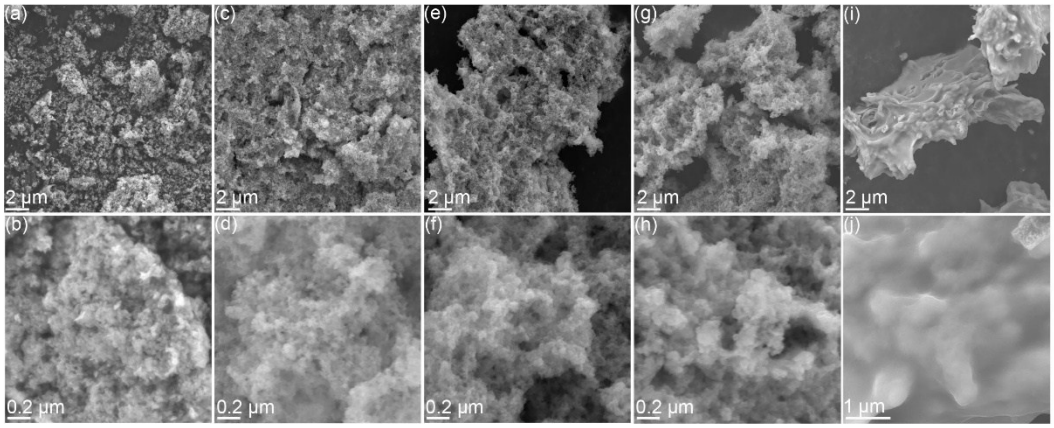


**Fig. S2** SEM images for morphology characterization. (a) and (b) for $MoS_2$, (c) and (d) for $MoS_2$-AC-20, (e) and (f) for $MoS_2$-AC-50, (g) and (h) for $MoS_2$-AC-100, (i) and (j) for $MoS_2$-AC-200.

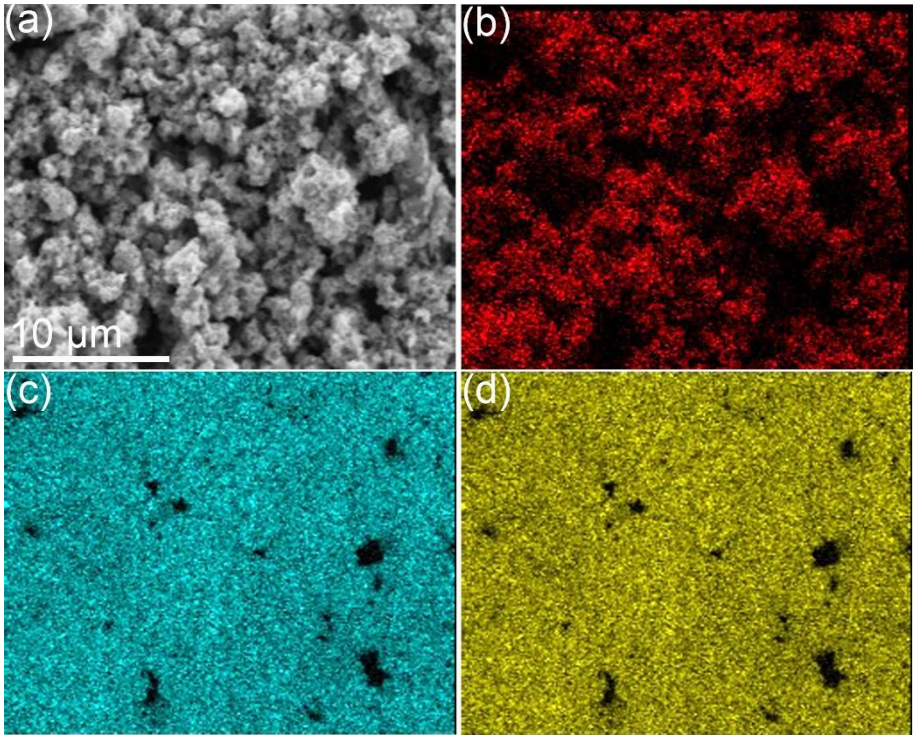


**Fig. S3** (a) SEM image of selected area for EDS test for $MoS_2$-PVP-100 and the corresponding element mappings: (b) C element, (c) Mo element and (d) S element.

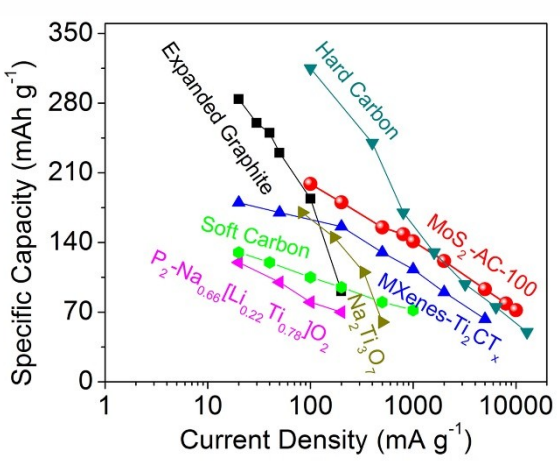


**Fig. S4** Rate capability for $MoS_2$-AC compared to other intercalated anodes in reported literatures: hard carbon,[S4] MXenes,[S5] expanded graphite,[S6] $Na_2Ti_3O_7$,[S7] $P_2$-$Na_{0.66}Li_{0.22}Ti_{0.78}O_2$,[S8] and soft carbon.[S9]

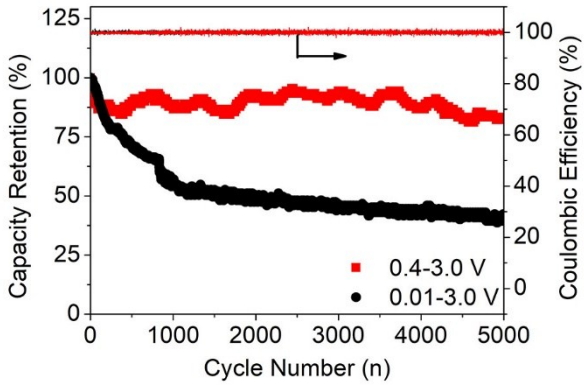


**Fig. S5** Long-term cycling performance of $MoS_2$-AC-100 at a current density of 5 A $g^{-1}$ within two potential ranges of 0.4-3.0 V and 0.01-3.0 V.

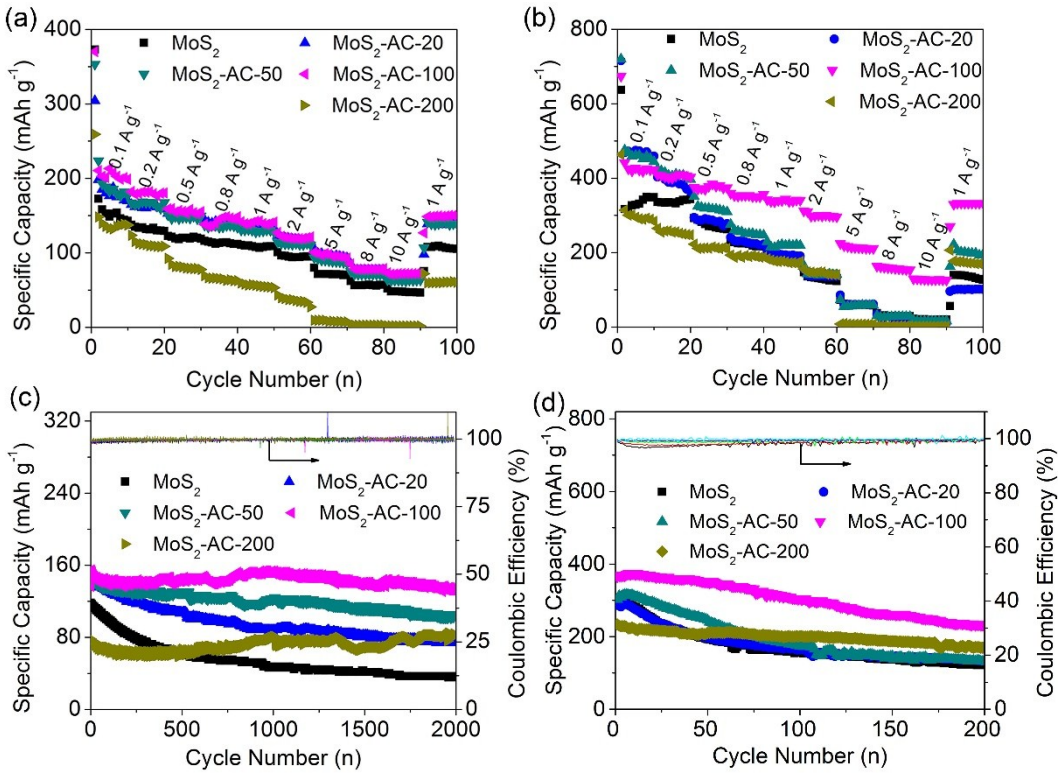


**Fig. S6** (a) Rate performance for $MoS_2$-AC electrodes at various current densities from 0.1 to 10 A $g^{-1}$ within a working potential range of 0.4-3.0 V. (b) Rate performance for $MoS_2$-AC electrodes at various current densities from 0.1 to 10 A $g^{-1}$ within a working potential range of 0.01-3.0 V. (c) and (d) Long-term cycling performance for $MoS_2$-AC electrodes at 1 A $g^{-1}$ within two working potential ranges: 0.4-3.0 V and 0.01-3.0 V, respectively.

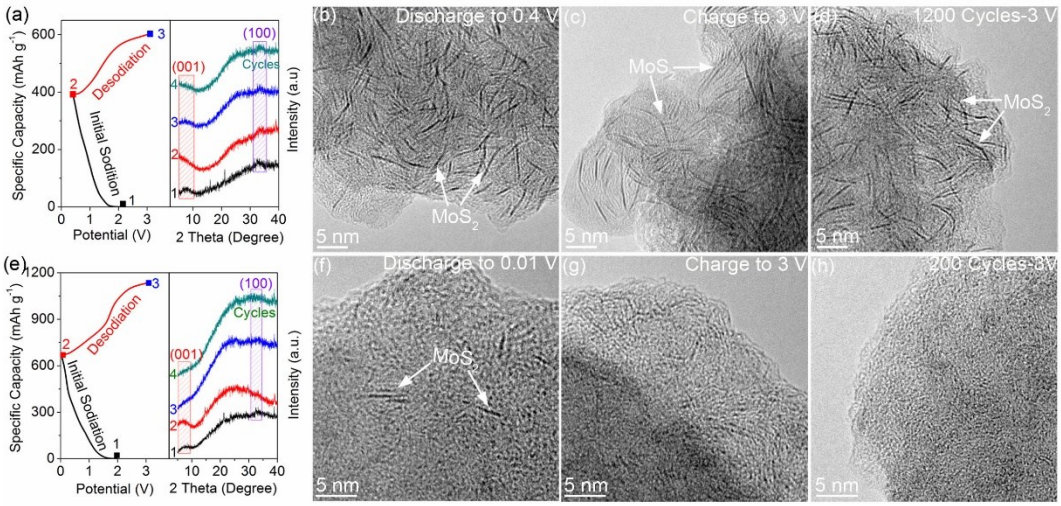


**Fig. S7** Initial charge/discharge process for $MoS_2$-AC-100 at a current density of 0.1 A $g^{-1}$ and the corresponding ex-situ XRD patterns for $MoS_2$-AC-100 during the cycles within two trade-off potentials: (a) 0.4 V and (e) 0.01 V. The notes: 1-pristine material, 2-initial sodiation, 3-initial desodiation. The note for 4 is the desodiated state after long cycles of 1200 cycles for (a) and 200 cycles for (b) at a current density of 1 A $g^{-1}$. HRTEM images of $MoS_2$-AC-100 sample cycled within 0.4-3.0 V: (b) the initial sodiation to 0.4 V (*vs.* $Na/Na^+$), (c) initial desodiation to 3.0 V (*vs.* $Na/Na^+$), (d) 1200$^{th}$ cycle to 3.0 V (*vs.* $Na/Na^+$). HRTEM images of $MoS_2$-AC-100 sample cycled within 0.01-3.0 V: (f) the initial sodiation to 0.01 V (*vs.* $Na/Na^+$), (g) initial desodiation to 3.0 V (*vs.* $Na/Na^+$), (h) 200$^{th}$ cycle to 3.0 V (*vs.* $Na/Na^+$). The current density is 0.1 A $g^{-1}$, except for 1 A $g^{-1}$ for long cycles for (d) and (h).

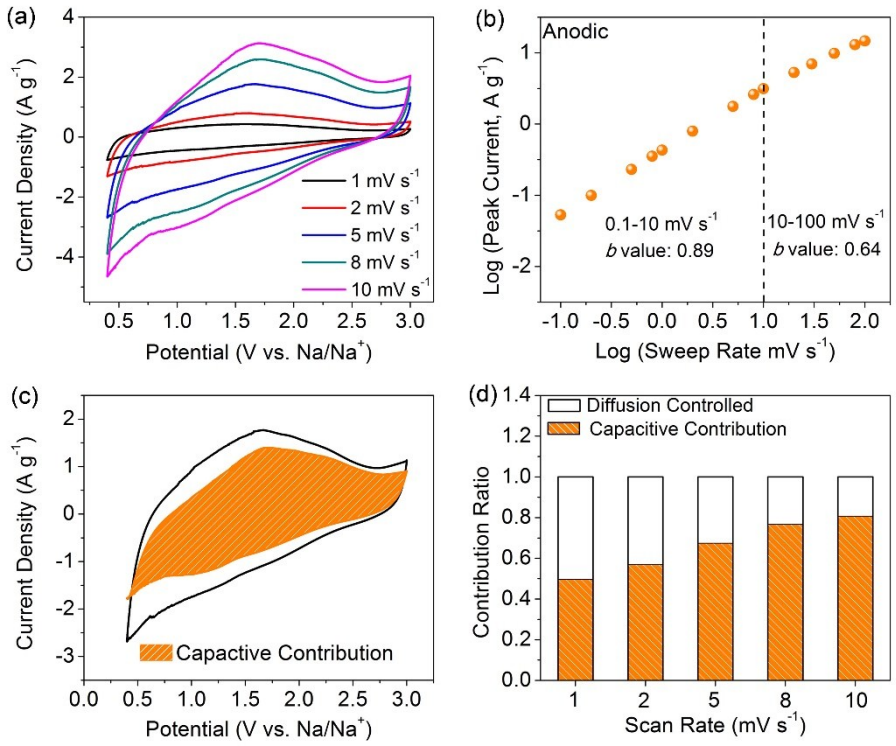


**Fig. S8** Electrochemical kinetics analysis of $MoS_2$-AC-100 electrode. (a) CV curves at various scan rates from 1 to 10 mV $s^{-1}$. (b) Determination of the *b*-value using the relationship between anodic peak current and scan rate. (c) Separation of the capacitive and diffusion currents at a scan rate of 5 mV $s^{-1}$, respectively. (d) Contribution ratio of the capacitive charge versus scan rate.

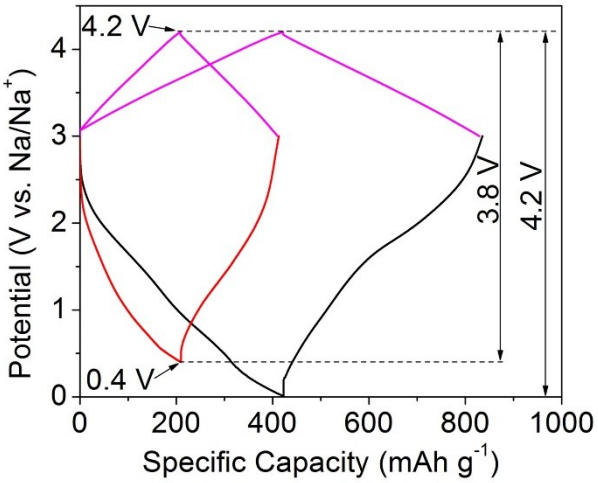


**Fig. S9** Charge/discharge curves of $MoS_2$-AC-100 within two different potential windows (0.4-3.0 V (red line) and 0.01-3.0 V (black line)) and PDPC versus $Na/Na^+$, respectively. The specific current density is 1 A $g^{-1}$.

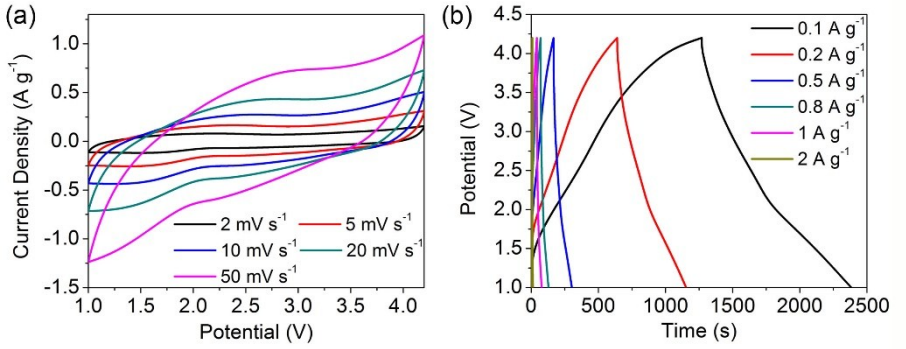


**Fig. S10** (a) CVs of as-fabricated $MoS_2$-AC//PDPC-4.2 V at various scan rates from 2 to 50 mV $s^{-1}$. (b) Charge/discharge curves of as-fabricated $MoS_2$-AC//PDPC-4.2 V SIC at the different current densities from 0.1 to 2 A $g^{-1}$.

**References**

S1 H. Ye, L. Wang, S. Deng, X. Zeng, K. Nie, P. N. Duchesne, B. Wang, S. Liu, J. Zhou, F. Zhao, N. Han, P. Zhang, J. Zhong, X. Sun, Y. Li, Y. Li and J. Lu, *Adv. Energy Mater*. 2016, **6**, 1601602.

S2 W. Zhang, T. Zhou, J. Zheng, J. Hong, Y. Pan and R. Xu, *ChemSusChem* 2015, **8**, 1464-1471.

S3 A. M. Abdelghany, M. S. Mekhail, E. M. Abdelrazek and M. M. Aboud, *J. Alloys Compd.* 2015, **646**, 326-332.

S4 J. Ding, H. Wang, Z. Li, K. Cui, D. Karpuzov, X. Tan, A. Kohandehghan and D. Mitlin, *Energy Environ. Sci.* 2015, **8**, 941-955.

S5 X. Wang, S. Kajiyama, H. Iinuma, E. Hosono, S. Oro, I. Moriguchi, M. Okubo and A. Yamada, *Nat. Commun.* 2015, **6**, 6544.

S6 Y. Wen, K. He, Y. Zhu, F. Han, Y. Xu, I. Matsuda, Y. Ishii, J. Cumings and C. Wang, *Nat. Commun.* 2014, **5**, 4033.

S7 A. Rudola, K, Saravanan, C. W. Masona and Palani Balaya, *J. Mater. Chem. A* 2013, **1**, 2653–2662.

S8 Y. Wang, X. Yu, S. Xu, J. Bai, R. Xiao, Y. –S. Hu, H. Li, X. –Q. Yang, L. Chen and X. Huang, *Nat. Commun.* 2013, **4**, 2365.

S9 W. Luo, Z. Jian, Z. Xing, W. Wang, C. Bommier, M. M. Lerner and X. Ji, *ACS Cent. Sci.* 2015, **1**, 516−522.